Journal of Medicinal Chemistry

ARTICLE

pubs.acs.org/jmc

Rational Design of Potent, Small, Synthetic Allosteric Inhibitors of Thrombin

Preetpal Singh Sidhu,[†,‡] Aiye Liang,[†,‡] Akul Y. Mehta,[†,‡] May H. Abdel Aziz,[†,‡] Qibing Zhou,[†,§] and Umesh R. Desai*[,†,‡]

[†]Department of Medicinal Chemistry and [‡]Institute for Structural Biology and Drug Discovery, Virginia Commonwealth University, Richmond, Virginia 23219, United States

[§]Institute for Materia Medica, College of Life Science and Technology, Huazhong University of Science and Technology, Wuhan, Hubei 430074, P. R. China

Supporting Information

ABSTRACT: Thrombin is a key enzyme targeted by the majority of current anticoagulants that are direct inhibitors. Allosteric inhibition of thrombin may offer a major advantage of finely tuned regulation. We present here sulfated benzofurans as the first examples of potent, small allosteric inhibitors of thrombin. A sulfated benzofuran library of 15 sulfated monomers and 13 sulfated dimers with different charged, polar, and hydrophobic substituents was studied in this work. Synthesis of the sulfated benzofurans was achieved through a multiple step, highly branched strategy, which culminated with microwave-assisted chemical sulfation. Of the 28 potential inhibitors, 11 exhibited reasonable inhibition of human α-thrombin at pH 7.4. Structure−activity relationship analysis indicated that sulfation at the 5-position of the benzofuran scaffold was essential for targeting thrombin. A *tert*-butyl 5-sulfated benzofuran derivative was found to be the most potent thrombin inhibitor with an IC_{50} of 7.3 μM under physiologically relevant conditions. Michaelis−Menten studies showed an allosteric inhibition phenomenon. Plasma clotting assays indicate that the sulfated benzofurans prolong both the activated partial thromboplastin time and prothrombin time. Overall, this work puts forward sulfated benzofurans as the first small, synthetic molecules as powerful lead compounds for the design of a new class of allosteric inhibitors of thrombin.

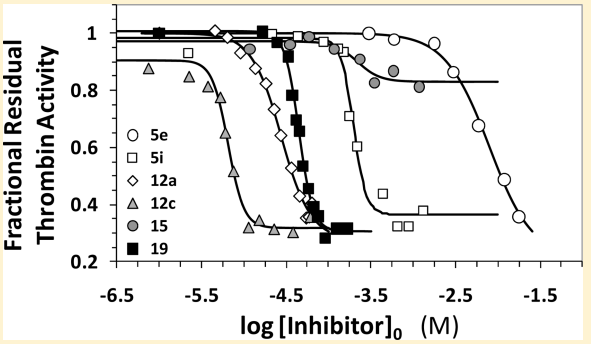

INTRODUCTION

Thrombin is a key enzyme of the coagulation cascade exhibiting important roles in both procoagulation and anticoagulation processes. Most clinically used anticoagulant drugs, including polymeric heparin, warfarin, hirudin, argatroban, and the recently approved dabigatran aim to reduce thrombin activity.[1−3] Although these drugs have been successful in treating many thrombotic disorders, the anticoagulation therapy continues to suffer from bleeding risk, narrow therapeutic index, and other drug-specific adverse effects, which highlight the critical need to develop agents with better therapeutic profile.

Structurally, thrombin is a complex serine protease of the trypsin family that displays multiple ligand-binding domains, which modulate its activity and interactions with other molecules. These domains include the active site, anion-binding exosites I and II, and the sodium binding site. The design of thrombin inhibitors has focused almost exclusively on blocking the substrate's access to the active site through a competitive process.[3] This paradigm has resulted in the design of thousands of molecules distributed across a large number of scaffolds.[3−6] Of these, a select group of scaffolds, including the pyrazoles, napthylamidines, indoles, biphenyls, and benzimidazoles, are preferred because of their high thrombin selectivity. Fundamentally, these designed inhibitors attempt to mimic the D-Phe-Pro-Arg recognition sequence through the incorporation of a guanidine or amidine moiety. Recently, however, newer molecules have been designed with a P-1 halophenyl substituent to interact with Tyr228 in the S1 pocket to improve the poor oral bioavailability of most P-1 guanidine-based inhibitors.[3,7−9]

An exciting alternative to competitive inhibition of thrombin is allosteric inhibition through either exosite I or exosite II. It is well established that binding of ligands in these exosites can induce conformational changes in the active site of thrombin.[10−13] An example of this is thrombomodulin, which interacts with exosite I to change the substrate specificity of thrombin from fibrinogen to protein C.[12] Likewise, hirugen binding in exosite I increases or decreases the catalytic efficiency of thrombin, depending on the nature of the chromogenic substrate.[10,11] Similarly, exosite I−active site allosteric coupling is also the reason why peptides such as

Received: May 6, 2011
Published: June 29, 2011

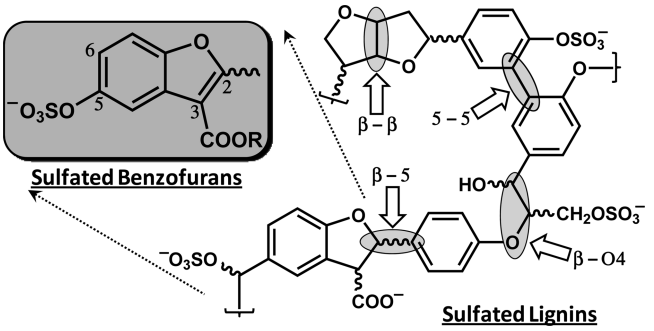

Figure 1. Design of sulfated benzofurans on the basis of the structure of sulfated lignins, which were found to be potent inhibitors of thrombin. Sulfated lignins are a three-dimensional network of chemoenzymatically coupled 4-hydroxycinnamic acid monomers. Four different intermonomeric linkages are possible in these oligomers including $\beta-5$, $\beta-$O4, $\beta-\beta$, and 5−5 linkages. Chiral centers are identified using curvy bonds. The chain length of sulfated lignins is typically 5−15 monomer units. Sulfated benzofurans studied in this work were designed from one specific structure generated by $\beta-5$ linked monomers, as shown by the structure in box. Positions 2, 3, 5, and 6 are numbered. See text for details.

bothrojaracin inhibit thrombin.[14,15] Nevertheless, no small organic molecule has been designed that utilizes exosite I to effect physiological thrombin inhibition.

Exosite II ligands include heparin, chondroitin sulfate, haemadin, and fibrinogen γ'. These can be broadly classified as either highly anionic polysaccharides or traditional peptides. Interaction of heparin with exosite II is known to induce greater reactivity with antithrombin, and recent work shows that formation of antithrombin−thrombin complex disrupts exosite II.[16] Also, exosite II−active site coupling is suggested by the change in fluorescence properties of para-aminobenzamidine, a noncovalent active site probe, upon heparin binding to exosite II.[17] However, no exclusive exosite II ligand has been found to date that reduces the catalytic efficiency of thrombin.

Allosteric regulation is a promising strategy for thrombin inhibition. Nature tends to utilize allosterism to confer specificity of recognition and also to effect regulation. For thrombin, the possibility of regulation, or controlled inhibition, is of considerable importance because nearly all current anticoagulants are associated with risk of bleeding. An appropriately designed allosteric regulator that does not fully nullify the procoagulant signal may maintain a finely tuned balance between procoagulant and anticoagulant signal, resulting in reduced bleeding complications. In pursuit of such allosteric regulators, we had earlier designed sulfated low molecular weight lignins (LMWLs) as functional mimetics of heparin targeted to exosite II-like regions of coagulation enzymes, including thrombin.[18,19] Sulfated LMWLs, chemoenzymatic variants of the naturally available lignin (Figure 1), were found to potently inhibit thrombin with an IC_{50} of 18−34 nM under physiological conditions.[18] More importantly, sulfated LMWLs also inhibited blood clotting under ex vivo conditions with potency comparable to that of the LMW heparins.[20]

Despite their excellent in vitro and ex vivo anticoagulant properties, sulfated LMWLs are challenging because of their polydispersity and microheterogeneity, which parallel that observed with the heparins. Sulfated LMWLs represent a large library of structures arising from multiple intermonomeric linkages, variable sulfation and chain length, and the presence of many chiral centers (Figure 1).[21] These variables introduce considerable structural diversity to these molecules, which nevertheless bind to exosite II of thrombin and allosterically induce thrombin inhibition.[18] Sulfated LMWLs represent the first examples of an exclusive exosite II-mediated inhibition of the key coagulation protease.

In this work, we present a study of 28 monomeric and dimeric sulfated benzofurans, molecules derived from the sulfated LMWL structure, as inhibitors of thrombin. Enzyme inhibition studies show that the molecules display a range of inhibition potential, while Michaelis−Menten kinetic studies show the inhibition to arise from an allosteric process. Collectively, this work establishes the potential of allosteric inhibition of thrombin through the interesting and unusual features of sulfated benzofurans that direct the interaction with thrombin.

EXPERIMENTAL PROCEDURES

Chemicals, Reagents, and Analytical Chemistry. Microwave-based sulfation reactions were performed using a CEM-Discover synthesizer (Matthews, NC) in sealed reaction vessels (7 mL) at 50 W. The temperature of the reaction was maintained at the desired setting using cooled nitrogen (45 psi) flow. Reagents and chemicals used in reactions were purchased from either Sigma-Aldrich (Milwaukee, WI) or Fisher (Pittsburgh, PA) and used as supplied. Analytical thin layer chromatography (TLC) was performed using UNIPLATE silica gel GHLF 250 μm precoated plates (ANALTECH, Newark, DE) that were analyzed by fluorescence (254 nm). Compound purity was evaluated independently through gradient reverse-phase HPLC. The purity of each compound synthesized in this work was greater than 95% and is listed in the Supporting Information.

Column chromatography was performed using Teledyne ISCO (Lincoln, NE) Combiflash RF system and disposable normal silica cartridges of 30−50 μm particle size, 230−400 mesh size, and 60 Å pore size. Sodium exchange chromatography was performed using SP Sephadex C-25 sodium cation exchange columns from GE Healthcare Life Sciences (Piscataway, NJ). Approximately 100 mg of sulfated sample was loaded onto 10 g of the cation exchanger in a 10 mm × 460 mm column and eluted with either water or 20% EtOH/H_2O at 0.5 mL/min. Anhydrous reactions were carried out under nitrogen atmosphere in glassware dried at high temperature. Reagent solutions and solvents were handled under nitrogen atmosphere using syringe techniques. HPLC purification of sulfated benzofurans was carried out on a Jasco chromatography system (Easton, MD) using a 250 mm × 10 mm Varian's Dynamax Microsorb C4 column. An acetonitrile−water gradient (5−100% acetonitrile in 20 min) at 3 mL/min was used to purify the compounds on milligram scale. The eluents were detected at 300 nm.

^{1}H and ^{13}C NMR spectra were recorded at either 300 or 400 MHz (Varian Mercury or Bruker Ultrashield Plus) in appropriate deuterated solvents including $CDCl_3$, DMSO-d_6, CD_3OD, acetone-d_6, or D_2O. All signals are reported in ppm with the internal chloroform, DMSO, acetone, and D_2O signals at 7.26, 2.50, 3.31, 2.05, and 4.79, respectively, as standards. The data are reported as chemical shifts (ppm), multiplicity (s = singlet, d = doublet, t = triplet, m = multiplet), coupling constant(s) (Hz), and integration. Mass spectrometry was performed on all synthesized molecules using a Micromass ZMD4000 single quadrupole mass spectrometer with ESI ionization probe operating in negative ion mode (Waters Corp., Milford, MA). The samples, dissolved in acetonitrile containing formic acid (5% v/v), were infused at 10 μL/min. The source block temperature and the probe temperature were typically held at 100 and 120 °C, respectively, while corona and cone voltages were selected through manual optimization. The desolvation nitrogen flow was 500 L/h. Mass spectra were acquired in the mass range from 110 to 1000 Da at 400 amu/s.

Synthesis of Benzofuran Monomer and Dimer Precursors for Subsequent Sulfation at 5-, 5′-, and Other Positions. The

detailed protocol for the synthesis of each benzofuran precursor is provided in Supporting Information. The reactions used in the synthesis are fairly common and hence not described here.

Sulfation of Appropriate Precursors To Yield Sulfated Benzofuran Monomers and Dimers. The synthesis of sulfated benzofurans was developed following our earlier report on the synthesis of sulfated flavonoids.[22] Briefly, to a solution of unsulfated benzofuran monomer or dimer (typically 50 mg) in acetonitrile/DMF (4:1, 0.45 mL) in a microwave tube were added triethylamine (10 equiv) and trimethylamine−sulfur trioxide complex (15 equiv). The reaction mixture was exposed to microwaves (50 W) for 40 min at 100 °C followed by vacuum concentration to remove all solvent. The solid so obtained was directly loaded on a Sephadex C-25 cation exchange resin and eluted with water. Fractions containing the sulfated product were lyophilized to obtain a solid residue, which was further purified on reverse-phase gradient HPLC to remove residual unsulfated contaminants.

5a: ^{1}H NMR (D_2O, 400 MHz) δ 1.45 (t, J = 6 Hz, 3H), 2.51 (s, 3H), 3.76 (s, 3H), 4.36 (q, J = 6 Hz, 2H), 5.38 (s, 1H), 7.15 (s, 1H), 7.57 (s, 1H).

5b: ^{1}H NMR (D_2O, 400 MHz) δ 2.48 (s, 3H), 3.89 (s, 3H), 4.21 (s, 3H), 6.98 (s, 1H), 6.61 (s, 1H). ESI MS (−*ve*) m/z calcd for $C_{12}H_{11}O_8SNa$ [$(M - Na)^-$)] 315.02, found 315.01$(M - Na)^-$.

5c: ^{1}H NMR (D_2O, 400 MHz) δ 1.62 (s, 9H), 2.49 (s, 3H), 3.89 (s, 3H), 6.98 (s, 1H), 6.61 (s, 1H). ^{13}C NMR (D_2O) δ 13.40, 21.22, 61.33, 73.87, 99.93, 107.79, 114.00, 118.54, 139.23, 147.28, 150.45, 164.37, 165.49. ESI MS (−*ve*) m/z calcd for $C_{13}H_{17}O_8SNa$ [$(M - Na)^-$)] 357.05, found 357.08 $(M - Na)^-$.

5d: ^{1}H NMR (D_2O, 400 MHz) δ 2.48 (s, 3H), 3.21 (s, 3H), 3.62 (t, J = 12 Hz, 2H), 3.72 (s, 3H), 4.26 (t, J = 12 Hz, 2H), 6.91 (s, 1H), 7.59 (s, 1H). ESI MS (−*ve*) m/z calcd for $C_{13}H_{13}O_9SNa$ [$(M - Na)^-$)] 345.02, found 345.01 $(M - Na)^-$.

5e: ^{1}H NMR (D_2O, 400 MHz) δ 1.70 (m, 6H), 2.99 (s, 3H), 4.41 (q, J = 17 Hz, 2H), 4.66 (q, J = 17 Hz, 2H), 7.55 (s, 1H), 8.21 (s, 1H). ^{13}C NMR (D_2O) δ 16.36, 16.39, 16.76, 63.15, 67.53, 99.69, 110.66, 116.09, 119.96, 141.73, 146.05, 151.33, 152.58, 165.90, 167.00. ESI HRMS (−*ve*) m/z calcd for $C_{14}H_{16}O_8SNa$ [$(M - Na)^-$)] 343.0512, found 343.0357 $(M - Na)^-$.

5f: ^{1}H NMR (D_2O, 400 MHz) δ 1.37 (m, 9H), 2.36 (s, 3H), 4.23 (q, J =18 Hz, 2H), 4.54 (m, 1H), 6.96 (s, 1H), 7.60 (s, 1H). ^{13}C NMR (D_2O) δ 13.40, 13.48, 21.22, 61.33, 73.87, 99.93, 107.79, 114.00, 118.54, 139.23, 147.28, 150.45, 164.37, 165.49. ESI HRMS (−*ve*) m/z calcd for $C_{14}H_{15}O_8SNa$ [$(M - Na)^-$)] 357.0532, found 357.0600 $(M - Na)^-$.

5g: ^{1}H NMR (D_2O, 400 MHz) δ 1.45 (t, J =18 Hz, 3H), 2.50 (s, 3H), 3.64 (s, 3H), 4.31 (q, J = 18 Hz, 2H), 5.33 (s, 2H), 7.15 (s, 1H), 7.64 (s, 1H). ESI HRMS (−*ve*) m/z calcd for $C_{14}H_{15}O_9SNa$ [$(M - Na)^-$)] 359.0420, found 359.0395 $(M - Na)^-$.

5h: ^{1}H NMR (D_2O, 400 MHz) δ 1.39 (t, J =18 Hz, 3H), 2.57 (s, 3H), 3.87 (m, 8H), 4.29 (q, J =18 Hz, 2H), 7.45 (s, 1H), 7.57 (s, 1H). ^{13}C NMR (D_2O) δ 13.48, 13.72, 44.11, 44.94, 61.53, 61.58, 66.25, 105.77, 106.60, 108.11, 114.53, 123.18, 139.99, 140.26, 149.66, 154.36, 165.33, 166.19. ESI HRMS (−*ve*) m/z calcd for $C_{17}H_{18}O_{10}SNa$ [$(M - Na)^-$)] 428.0332, found 428.0889 $(M - Na)^-$.

5i: ^{1}H NMR (D_2O, 400 MHz) δ 2.51 (s, 3H), 3.63 (s, 3H), 4.65 (d, 2H), 5.02 (d, 1H), 5.16 (d, 2H), 5.91 (m, 1H), 6.81 (s. 1H), 7.56 (s, 1H). ^{13}C NMR (D_2O) δ 13.40, 55.05, 61.19, 70.68, 97.79, 107.91, 113.75, 114.30, 118.36, 128.61, 128.99, 138.55, 148.09, 150.16, 158.52, 163.59, 165.06. ESI HRMS (+ve) m/z calcd for $C_{20}H_{19}O_9SNa$ [$(M + Na)^+$)] 481.0632, found 481.1400 $(M + Na)^+$.

5j: ^{1}H NMR (D_2O, 400 MHz) δ 1.28 (t, J =18 Hz, 3H), 2.09 (s, 3H), 3.54 (s, 3H), 4.12 (q, J = 18 Hz, 2H), 4.78 (s, 2H), 6.57 (s, 1H), 6.68 (d, J = 21 Hz, 2H), 7.17 (d, J = 21 Hz, 2H), 7.67 (s,1H). ^{13}C NMR (D_2O) δ 13.40, 55.05, 61.19, 70.68, 97.79, 107.91, 113.75, 114.30, 118.36, 128.61, 128.99, 138.55, 148.09, 150.16, 158.23, 163.59, 165.06. ESI MS (−*ve*) m/z calcd for $C_{14}H_{13}O_8SNa$ [$(M - Na)^-$)] 325.03, found 325.04 $(M - Na)^-$.

6: ^{1}H NMR (CD_3OD, 300 MHz) δ 2.61 (s, 3H), 3.86 (s, 3H), 6.88 (s, 2H), 7.15 (s, 1H), 7.86 (s, 1H). ^{13}C NMR (CD_3OD) δ 10.85, 55.78, 59.93, 95.76, 110.69, 112.67, 120.71, 138.55, 150.48, 151.65, 154.22.

7: ^{1}H NMR (CD_3OD, 300 MHz) δ 0.44 (s, 6H), 1.02 (s, 9H), 2.75 (s, 3H), 3.96 (s, 3H), 6.68 (s, 2H), 6.98 (s, 1H), 7.36 (s, 1H). ^{13}C NMR (CD_3OD) δ 4.48, 12.29, 18.70, 26.02, 55.88, 56.04, 95.47, 109.94, 114.31, 120.84, 142.03, 149.32, 149.40, 151.81.

9a: ^{1}H NMR (D_2O, 400 MHz) δ 2.47 (S, 3H), 3.55−3.90 (m, 8H), 3.91 (s, 3H), 7.25 (s, 1H), 7.41 (s, 1H). ^{13}C NMR (D_2O, 400 MHz) δ 12.48, 42.76, 47.82, 56.43, 66.41, 66.79, 96.68, 110.52, 112.70, 118.31, 137.35, 149.74, 151.36, 156.79, 166.23. ESI HRMS (−*ve*) m/z calcd for $C_{15}H_{16}NO_8SNa$ [$(M - Na)^-$)] 370.0544, found 370.0652 $(M - Na)^-$.

9b: ^{1}H NMR (D_2O, 400 MHz) δ 0.89 (d, J = 17 Hz, 3H), 1.01 (m, 1H), 1.61−1.81 (m, 4H), 2.39 (s, 3H), 2.92 (m, 1H), 3.08 (m, 1H), 3.56 (m, 1H), 3.92 (s, 3H), 4.45 (m, 1H), 7.27 (s, 1H), 7.64 (s, 1H). ^{13}C NMR (D_2O) δ 12.47, 12.55, 14.88, 20.89, 30.17, 55.67, 56.59, 96.67, 111.46, 112.63, 118.67, 137.67, 149.82, 151.26, 155.45, 165.32. ESI HRMS (−*ve*) m/z calcd for $C_{17}H_{20}NO_7SNa$ [$(M - Na)^-$)] 482.1022, found 382.0847 $(M - Na)^-$.

10: ^{1}H NMR (D_2O, 400 MHz) δ 1.47 (t, J =18 Hz, 3H), 2.71 (m, 4H), 3.81 (m, 4H), 3.95 (s, 3H), 4.02 (s, 2H), 4.39 (q, J = 18 Hz, 2H), 7.25 (s, 1H), 7.74 (s, 1H). ^{13}C NMR (D_2O) δ 13.45, 52.47, 52.64, 56.34, 61.82, 66.07, 96.24, 111.83, 114.82, 117.14, 137.95, 150.45, 151.64, 159.30, 164.77. ESI HRMS (−*ve*) m/z calcd for $C_{17}H_{20}NO_9SNa$ [$(M - Na)^-$)] 414.0933, found 414.0847 $(M - Na)^-$.

12a: ^{1}H NMR (CD_3OD, 300 MHz) δ 1.32 (J = 6 Hz, t, 3H), 2.65 (s, 3H), 3.82 (s, 3H), 3.86 (s, 3H), 4.29 (J = 6 Hz, q, 2H), 5.52 (s, 2H), 7.12 (s, 1H, Ar−H), 7.22 (s, 1H, Ar−H), 7.43 (s, 1H, Ar−H), and 8.04 (s, 1H, Ar−H). ^{13}C NMR (CD_3OD) δ 13.12, 13.53, 13.54, 55.65, 60.20, 60.67, 63.93, 95.54, 95.63, 109.19, 112.32, 115.57, 117.40, 118.31, 139.89, 145.50, 149.74, 152.08, 152.20, 158.70, 162.67, 163.51, 164.48. ESI HRMS (−*ve*) m/z calcd for $C_{26}H_{25}O_{13}SNa$ [$(M - Na)^-$)] 577.1011, found 577.1146 $(M - Na)^-$.

12b: ^{1}H NMR (CD_3OD, 300 MHz) δ 2.67 (s, 3H), 3.83 (s, 3H), 3.84 (s, 3H), 3.85 (s, 3H), 3.86 (s, 3H), 5.55 (s, 2H), 7.13 (s, 1H), 7.24 (s, 1H), 7.47 9s, 1H), 8.03 (s, 1H). ESI HRMS (−*ve*) m/z calcd for $C_{24}H_{21}O_{13}SNa$ [$(M - Na)^-$)] 549.0723, found 549.0795 $(M - Na)^-$.

12c: ^{1}H NMR (CD_3OD, 300 MHz) δ 1.49 (s, 9H), 1.51 (s, 9H), 2.65 (s, 3H), 3.83 (s, 3H), 3.88 (s, 3H), 5.47 (s, 2H), 7.12 (s, 1H), 7.22 (s, 1H), 7.37 (s, 1H), 8.09 (s, 1H). ^{13}C NMR (CD_3OD) δ 13.09, 27.30, 27.45, 55.59, 55.66, 64.26, 81.00, 81.62, 95.44, 95.56, 109.89, 110.21, 113.55, 115.59, 117.70, 118.42, 139.79, 145.31, 149.83, 151.87, 152.05, 158.16, 162.26, 162.63, 163.80. ESI MS (−*ve*) m/z calcd for $C_{30}H_{33}O_{13}SNa$ [$(M - Na)^-$)] 633.16, found 633.19 $(M - Na)^-$.

12d: ^{1}H NMR (D_2O, 400 MHz) δ 2.30 (s, 3H), 3.26 (s, 3H), 3.32 (s, 3H), 3.57 (m, 2H), 3.63 (m, 5H), 3.77 (s, 3H), 4.18 (m, 2H), 4.27 (m, 2H), 5.17 (s, 2H), 6.49 (s, 1H), 6.89 (s, 1H), 6.93 (s, 1H), 7.67 (s, 1H). ^{13}C NMR (D_2O) δ 13.49, 55.40, 56.07, 58.13, 58.24, 62.74, 62.96, 63.79, 69.76, 69.89, 93.22, 95.76, 105.85, 107.40, 111.06, 114.98, 116.73, 117.17, 138.28, 144.55, 147.64, 148.10, 150.78, 151.62, 158.55, 162.96, 163.49, 164.40. ESI HRMS (−*ve*) m/z calcd for $C_{28}H_{29}O_{115}S$-Na [$(M - Na)^-$)] 637.1223, found 637.1161 $(M - Na)^-$.

12e: ^{1}H NMR (D_2O, 400 MHz) δ 1.14 (m, 12H), 2.32 (s, 3H), 3.72 (m, 4H), 4.06 (m, 4H), 5.15 (s, 2H), 6.51 9s, 1H), 6.71 9s, 1H), 6.98 (s, 1H), 7.56 (s, 1H). ESI HRMS (−*ve*) m/z calcd for $C_{28}H_{29}O_{13}SNa$ [$(M - Na)^-$)] 605.1312, found 605.0708 $(M - Na)^-$.

12f: ^{1}H NMR (D_2O, 400 MHz) δ 1.07 (m, 18H), 2.27 (s, 3H), 3.99 (m, 4H), 4.20 (m, 2H), 5.05 (s, 2H), 6.64 (s, 1H), 6.67 (s, 1H), 6.99 (s, 1H), 7.81 (s, 1H). ^{13}C NMR (D_2O) δ 13.29, 13.50, 13.69, 13.78, 20.94, 21.19, 21.40, 60.34, 61.09, 63.81, 71.86, 72.97, 98.90, 108.13, 111.04, 114.71, 117.74, 118.33, 139.92, 146.62, 146.72, 148.33, 148.60, 151.24, 158.69, 162.57, 163.34, 164.08. ESI HRMS (−*ve*) m/z calcd for $C_{30}H_{33}O_{13}SNa$ [$(M - Na)^-$)] 633.1236, found 633.1494 $(M - Na)^-$.

13: ^{1}H NMR (CD_3OD, 400 MHz) δ 1.38 (m, 6H,), 2.60 (m, 3H,), 3.71 (m, 4H,), 3.91 (s, 3H,), 3.93 (s, 3H), 4.37 (m, 6H,), 5.62 (s, 2H), 7.02 (s, 1H), 7.05 (s, 1H), 7.49 (s, 1H), 8.01 (s, 1H). ESI MS ($-ve$) m/z calcd for $C_{30}H_{32}NO_{14}SNa$ [$(M - Na)^-$)] 659.14, found 659.15 $(M - Na)^-$.

14: ^{1}H NMR (D_2O, 400 MHz) δ 2.40 (s, 3H,), 3.24 (m, 8H), 3.67 (m, 8H), 3.81 (s, 3H,), 3.92 (s, 3H), 5.30 (s, 2H,), 6.85 (s, 1H,), 7.14 (s, 1H), 7.33 (s.1H,), 7.43 (s, 1H). ^{13}C NMR (D_2O) δ 12.36, 42.55, 56.00, 56.40, 63.52, 66.17, 66.36, 96.23, 96.73, 107.16, 110.44, 113.33, 115.29, 116.94, 117.92, 138.10, 143.04, 148.81, 149.45, 151.21, 151.81, 152.46, 156.38, 164.20, 165.93. ESI HRMS ($-ve$) m/z calcd for $C_{30}H_{31}N_2O_{13}S$-Na [$(M - Na)^-$)] 659.1422, found 659.1531 $(M - Na)^-$.

17: ^{1}H NMR (D_2O, 400 MHz) δ 1.23 (m, 6H), 2.36 (s, 3H), 3.70 (s, 3H), 4.18 (m, 4H), 5.23 (s, 2H), 6.96 (s, 1H), 7.03 (s, 1H), 7.53 (s, 1H), 7.62 (s, 1H). ^{13}C NMR (D_2O) δ 13.4, 13.51, 13.59, 56.30, 61.53, 62.08, 63.51, 96.28, 99.06, 108.05, 111.73, 114.48, 115.06, 117.13, 119.54, 138.31, 138.82, 147.96, 150.23, 150.94, 152.02, 158.07, 164.50, 164.87, 165.60. ESI HRMS ($-ve$) m/z calcd for $C_{25}H_{22}O_{14}S_2Na$ [$(M - Na)^-$)] 665.0121, found 665.0366 $(M - Na)^-$.

18: ^{1}H NMR (D_2O, 400 MHz) δ 1.55 (t, J =18 Hz, 3H),1.59 (t, J =18 Hz, 3H), 2.41 (s, 3H), 3.81 (s, 3H), 4.18 (q, J =18 Hz, 2H), 4.23 (q, J =18 Hz, 2H), 5.18 (s, 2H), 6.71 (s, 1H), 6.89 (s, 1H), 7.65 (s, 1H), 7.91 (s, 1H). ^{13}C NMR (D_2O) δ 13.47, 13.61, 13.63, 56.32, 61.53, 62.18, 63.61, 96.28, 99.16, 108.01, 111.53, 114.48, 115.06, 117.13, 119.54, 138.31, 138.82, 147.96, 150.23, 150.84, 152.12, 158.17, 164.53, 164.77, 165.60. ESI HRMS ($-ve$) m/z calcd for $C_{25}H_{22}O_{14}S_2Na$ [$(M - Na)^-$)] 665.0121, found 665.0277 $(M - Na)^-$.

19: ^{1}H NMR ($CDCl_3$, 300 MHz) δ 1.39 (m, 6H), 2.67 (s, 3H), 3.85 (s, 3H), 3.88 (s, 3H), 4.36 (m, 4H), 5.55 (s, 2H), 7.22 (s, 1H), 7.23 (s, 1H), 7.43 (s, 1H), 8.07 (s, 1H). ^{13}C NMR (CD_3OD) δ 13.25, 13.38, 13.52, 55.66, 55.77, 60.25, 60.79, 63.16, 95.63, 99.17, 103.95, 108.76, 112.48, 115.58, 117.27, 120.11, 139.90, 146.40, 148.00, 148.45, 152.15, 152.23, 158.27, 163.04, 163.59, 164.61. ESI HRMS ($-ve$) m/z calcd for $C_{26}H_{25}O_{13}SNa$ [$(M - Na)^-$)] 577.1011, found 577.1100 $(M - Na)^-$.

Synthesis of Benzofuran Dimer 15 from 12a. To a solution of **12a** (100 mg, 0.16 mmol) in 2 mL of methanol was added LiOH (20 mg, 0.8 mmol), and the mixture was stirred for 5 h at room temperature. After completion, the reaction mixture was concentrated and purified using HPLC. δ ^{1}H NMR (CD_3OD, 300 MHz) δ 2.66 (s, 3H), 3.84 (s, 3H), 3.89 (s, 3H), 5.52 (s, 2H), 7.11 (s, 1H, Ar−H), 7.27 (s, 1H, Ar−H), 7.41 (s, 1H, Ar−H), and 8.01 (s, 1H, Ar−H). ^{13}C NMR (CD_3OD) δ 13.43, 61.67, 63.73, 95.54, 95.63, 109.19, 112.32, 115.57, 117.40, 118.31, 139.89, 145.50, 149.74, 152.08, 152.20, 158.54, 162.57, 164.51, 165.48. ESI HRMS ($-ve$) m/z calcd for $C_{17}H_{20}NO_9SNa$ [$(M - Na)^-$)] 521.0322, found 521.1496 $(M - Na)^-$.

Synthesis of Benzofuran Dimer 16 from 11a. To a solution of **11a** (200 mg, 0.32 mmol) in 10 mL of anhydrous THF was added $LiAlH_4$ (65 mg, 1.6 mmol), and the mixture was stirred for 6 h under nitrogen. After completion, the reaction was quenched by adding 30 mL of water and extracted with 100 mL of diethyl ether twice. The organic layer was concentrated and purified using gradient flash chromatography (0−50% ethyl acetate in hexane). The reduced form of **11a** was sulfated using the general sulfation procedure described above. ^{1}H NMR (CD_3OD, 300 MHz) δ 0.17 (s, 6H), 1.01 (s, 9H), 2.71 (s, 3H), 3.87 (s, 3H), 3.91 (s, 3H)), 5.51 (s, 2H), 6.65 (s, 2H), 6.69 (s, 2H), 7.01 (s, 1H, Ar−H), 7.04 (s, 1H,), 7.37 (s, 1H), 7.45 (s, 1H). ^{13}C NMR ($CDCl_3$) δ −4.47, 12.31, 18.70, 26.00, 55.45, 55.81, 55.94, 56.58, 94.60, 95.48, 103.35, 114.35, 118.34, 120.39, 121.24, 142.32, 142.65, 144.82, 148.21, 149.73, 152.05.

Thrombin and Chemicals for Biological Experiments. Human α-thrombin was from Haematologic Technologies (Essex Junction, VT). Stock solutions of thrombin were prepared in 20 mM sodium phosphate buffer, pH 7.4, containing 100 mM NaCl. Chromogenic substrate Spectrozyme TH was from American Diagnostica (Greenwich, CT). Citrated human plasma for coagulation time assays was purchased from Valley Biomedical (Winchester, VA). Thromboplastin and ellagic acid were obtained from Fisher Diagnostics (Middletown, VA).

Inhibition of Thrombin. Direct inhibition of thrombin by sulfated benzofuran derivatives was measured through a chromogenic substrate hydrolysis assay.[18,19] The buffer used in these experiments was 20 mM Tris-HCl buffer, pH 7.4, containing 100 mM NaCl, 2.5 mM $CaCl_2$, and 0.1% polyethylene glycol (PEG) 8000. Benzofuran derivatives (2−30 μL) at concentrations ranging from 4 μg/mL to 5 mg/mL were diluted with appropriate volume of assay buffer in PEG 20000-coated acrylic cuvettes at 25 °C. To this solution was added 5 μL of thrombin solution to give approximately 5 nM initial thrombin concentration. After 10 min of incubation, 20 μL of 1 mM Spectrozyme TH was rapidly added and the residual thrombin activity was measured from the initial rate of increase in absorbance at 405 nm. Relative residual thrombin activity at each concentration of the inhibitor was calculated from the ratio of thrombin activity in the presence and absence of inhibitor. Logistic eq 1 was used to fit the dose-dependence of residual proteinase activity to obtain the IC_{50} and the efficacy ΔY (=$Y_M - Y_0$) of inhibition.

$$Y = Y_0 + \frac{Y_M - Y_0}{1 + 10^{(\log[I]_0 - \log IC_{50})(HS)}} \quad (1)$$

In this equation, Y is the ratio of residual thrombin activity in the presence of inhibitor to that in its absence (fractional residual activity), Y_M and Y_0 are the maximum and minimum possible values of the fractional residual proteinase activity, IC_{50} is the concentration of the inhibitor that results in 50% inhibition of enzyme activity, and HS is the Hill slope, which was set constant at 1. A current version of SigmaPlot (SPSS, Inc., Chicago, IL) was used to perform nonlinear curve fitting in which Y_M, Y_0, and IC_{50} were allowed to float.

Michaelis−Menten Kinetics of Spectrozyme TH Hydrolysis. The initial rate of Spectrozyme TH hydrolysis by 5−10 nM thrombin was monitored from the linear increase in absorbance at 405 nm corresponding to less than 10% consumption of the substrate, as described earlier.[18,19] The initial rate was measured as a function of various concentrations of the substrate (10−600 μM) in the presence of fixed concentration of dimer **12a** (0−30 μM) in 20 mM Tris-HCl buffer, pH 7.4, at 37 °C. The data were fitted by Michaelis−Menten eq 2 to determine K_M and V_{MAX}.

$$V_i = \frac{V_{MAX}[S]}{K_M + [S]} \quad (2)$$

Prothrombin Time and Activated Partial Thromboplastin Time. Clotting time was measured in a standard one-stage recalcification assay with a BBL Fibrosystem fibrometer (Becton-Dickinson, Sparles, MD), as described previously.[20,21] For PT assays, thromboplastin was reconstituted according to manufacturer's directions and warmed to 37 °C. A 10 μL sample of the sulfated benzofuran, to give the desired concentration, was brought up to 100 μL with citrated human plasma, incubated for 30 s at 37 °C followed by addition of 200 μL prewarmed thromboplastin. Clotting time in the absence of an anticoagulant was determined using 10 μL of deionized water. For the APTT assay, 10 μL of inhibitor was mixed with 90 μL of citrated human plasma and 100 μL of prewarmed APTT reagent (0.2% ellagic acid). After incubation for 4 min, clotting was initiated by adding 100 μL of 25 mM $CaCl_2$ (37 °C) and time to clot noted. Each clotting assay was performed in duplicate. The data were fit to a quadratic trendline, which was used to determine the concentration of the inhibitor necessary to double the clotting time, 2 × APTT or 2 × PT.

RESULTS AND DISCUSSION

Design of the Sulfated Benzofuran Scaffold. Sulfated LMWLs, which recognize exosite II of thrombin, are based on an aromatic

scaffold, a scaffold dramatically different from the highly anionic polysaccharide scaffold of heparin.[21] Nevertheless, sulfated LMWLs retain one characteristic of heparin: structural complexity arising from the presence of multiple intermonomeric linkages, such as $\beta-5$, $\beta-\beta$, $\beta-O4$, and 5−5 (Figure 1). A simple calculation suggests that LMWL molecules as small as a tetramer can exhibit nearly 1400 distinct structures even if sulfation and inter-residue linkage are the only variables considered. To uncover distinct structures that may be the seat of anticoagulant activity, we visualized the lignin structure as concatenated, aromatic units instead of repetitions of 4-hydroxycinnamic acid monomers joined together through different inter-residue linkages. In this alternative analysis, oligomeric lignin can be considered as a combinatorial library of dihydrobenzofuran, phenoxypropanoic acid, biphenyl, and fused furan monomers (Figure 1). We reasoned that one or more of these aromatic units with appropriate sulfate groups could be the seat of thrombin recognition and inhibition.

To begin assessing the contribution of these individual aromatic units, we focused on the benzofuran unit, which is a common scaffold used in many synthetic studies. In a preliminary investigation, we had prepared a library of sulfated and carboxylated benzofuran monomers, of which a small group of molecules were found to inhibit thrombin, albeit with IC_{50} in the millimolar range. Interestingly, mechanistic studies had suggested allosteric inhibition by these molecules.[23] This promise led us to explore a more diverse set of sulfated benzofuran monomers and dimers as potential inhibitors of thrombin (Figure 2).

Overall Description of the Sulfated Benzofuran Library. The benzofuran unit of sulfated LMWLs contains substitutions at the 2, 3, and 5 positions (Figure 1). Of these, the 2 and 5 positions are utilized for intermonomeric linkage and the 3 position may bear a carboxylate or an alkylsulfate group. Considering these variations, charged, polar, and hydrophobic substitutions were engineered on this scaffold to obtain a structurally diverse library. Figure 2 describes the multimodal approach developed to synthesize 15 sulfated monomers and 13 sulfated dimers. This library reflects significant variations in (1) the number of negatively charged groups (one to three anions), (2) the positions of anionic and polar substitutions from the terminal to the center of the scaffold, (3) the size and nature of hydrophobic groups, and (4) inter-residue linkage geometry. A characteristic feature is that each member of the library is nearly fully water-soluble because of the presence of one or more sulfate groups, despite the primarily hydrophobic benzofuran backbone. This combination of water solubility and hydrophobicity has been known to introduce novel physicochemical characteristics in the sulfated lignin-based scaffold, e.g., higher than expected partition coefficient[24] and greater proportion of nonionic forces in binding to proteins.[25]

Synthesis of Sulfated Benzofuran Monomers. The first step in the synthesis of the library was the generation of base structures, 5,6-dihydroxybenzofuran-3-carboxylic acid esters (**1a**−**e**, Figure 2), from catechol in one step using oxidative Michael addition conditions following the report of Pei et al.[26] The reaction was strongly susceptible to substituent effects, which required extensive optimization of reaction conditions, especially the organic base, reaction time, and solvent. Eventually, products **1a**−**e** were obtained in reasonably good yields (50−65%). Monoalkylation or acylation of dihydroxybenzofurans **1** proceeded smoothly to selective 6-substituted derivatives **2a**−**j**. That the substitution occurred at the 6-position of the benzofuran ring was confirmed through two-dimensional nuclear Overhauser spectroscopy experiment (ROESY), which showed a correlation between the protons of the 3-alkyl ester and 6-alkoxy groups (not shown). The monomeric benzofurans **2a**−**j** so synthesized in two steps formed one major group of precursors for library construction. Another set of monomer precursors **3a**−**g** and **4a**−**g** were synthesized from **2a**−**j** through silyl protection and bromination, respectively (Figure 2).

Monosulfated benzofurans **5a**−**j** were prepared by direct sulfation of precursors **2a**−**j**. Phenolic molecules are typically more challenging to sulfate than alcoholic molecules.[27] We had previously developed a microwave-based sulfation protocol for introducing multiple sulfate groups in a crowded environment using triethylamine−sulfur trioxide complex at 100 °C.[22,23] This method gave good yields of monosulfated benzofurans **5a**−**j** in their ammonium salt forms, which were exchanged for sodium using a Sephadex C-25 exchange column. To test whether the number and location of sulfate groups on the benzofuran scaffold play a significant role in recognizing thrombin, we introduced a sulfate group at the 3-position also. Thus, benzofurans **2a** and **3a** were reduced with LAH and sulfated to yield **6** and **7**, respectively. However, both **6** and **7** were found to degrade within a couple of hours after dissolution in water at room temperature. The reason for the reduced aqueous stability of these 3-methylene sulfated benzofurans is not clear, although the dual combination of electron pull by sulfate groups and electron push by ring oxygen may be the cause of more rapid desulfation.

To assess the importance of the nature of the carbonyl group at the 3-position, silyl-protected benzofuran ester **3** was directly converted to morpholinyl and 4-methylpiperidinyl amides **8a** and **8b**, respectively, using a procedure reported by Weinreb and co-workers in the late 1970s.[28] Desilylation and sulfation gave monosulfated benzofuran amides **9a** and **9b** in excellent yields. Finally, 2-morpholino monomer **10** was prepared from **4a** to study the effect of varying the 2-substituent.

Synthesis of Sulfated Benzofuran Dimers. The construction of the library of dimers relied on the nucleophilic displacement of the allylic bromide at the 2 position by free phenolic group at the 5-position. The apparent simplicity of this reaction[29] and the availability of 10 nucleophilic monomers **2a**−**j** and 7 allylic bromides **4a**−**g** enticed us to construct a combinatorial library (Figure 2). However, the coupling was challenging on both synthesis and purification fronts. Steric crowding around both the nucleophile and the electrophile resulted in less than optimal yields (<50%) of **11a**−**f**. In addition, the synthesized dimers typically coeluted with monomers in a wide range of multisolvent systems, creating significant purification issues. We suspected that coelution may be occurring because of π-stacking at high concentrations. Thus, a higher yielding dimerization reaction was desirable, which was made possible through implementation of microwave coupling. By use of this strategy, silylated dimers **11a**−**f** were synthesized in excellent yields (>90%). These were then deprotected and sulfated to yield monosulfated benzofuran dimers **12a**−**f**. Likewise, monosulfated benzofuran dimers **13** and **14**, which contain a morpholine ring at the 2 and 3 positions, respectively, were synthesized starting from monomers **4a** and **8a**, respectively, through a series of silyl protection, allylic bromination, deprotection, nucleophilic coupling, and sulfation steps (Figure 2).

To evaluate the role of multiple anionic groups on the small hydrophobic scaffold, **12a** was hydrolyzed in alcoholic LiOH[30] to yield **15**, a monosulfated, dicarboxylated dimer. Likewise, **11a** was reduced with LAH and sulfated to yield **16**, which is a disulfated dimer, but as with monomers **6** and **7**, **16** was found to degrade rapidly in water. Finally, coupling of **4a** with **1a** followed by

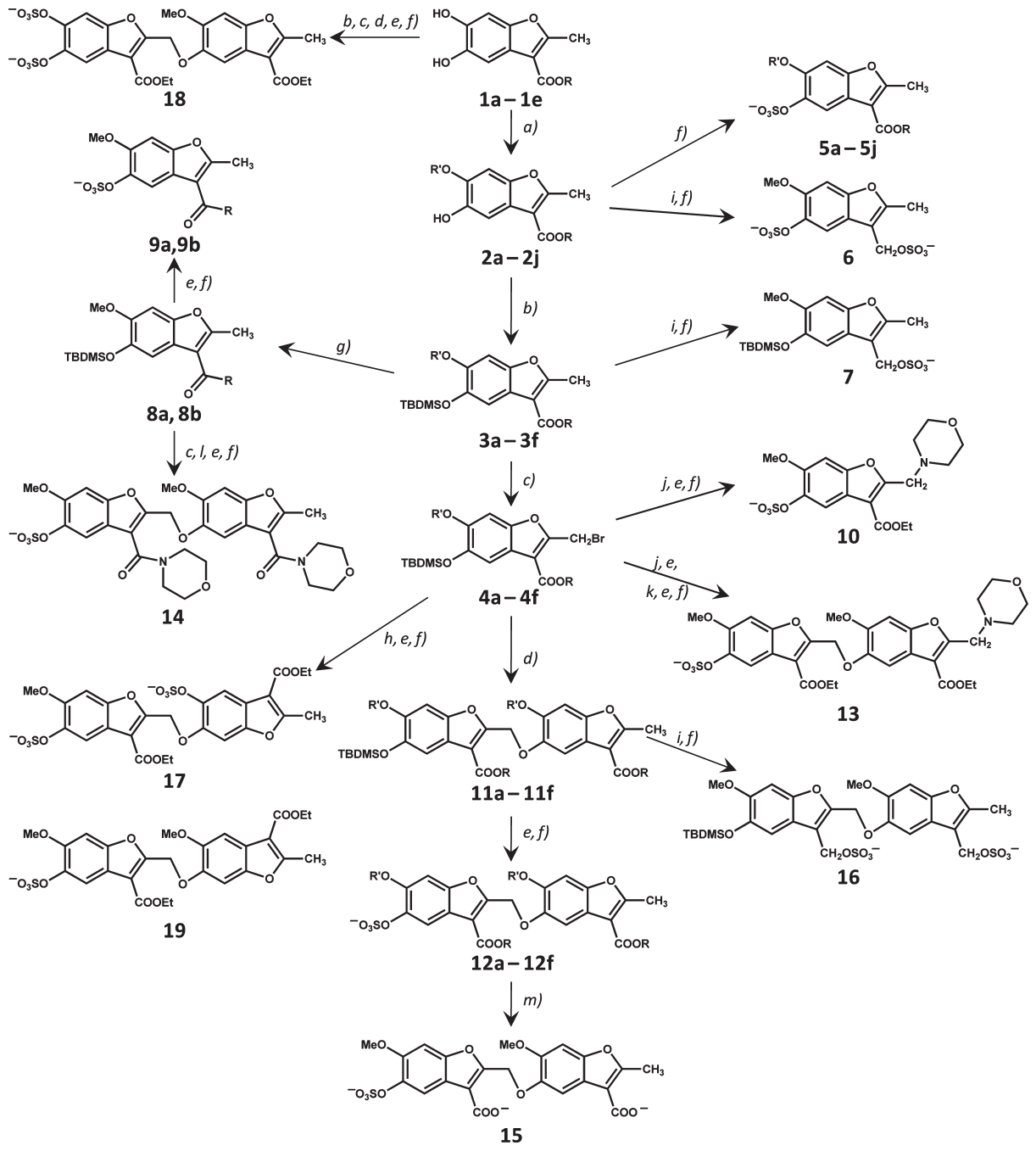

Figure 2. Synthesis of a library of sulfated benzofurans as potential allosteric regulators of thrombin. The library consists of 15 monomers (**5a**−**j**, **6**, **7**, **9a**, **9b**, and **10**) and 13 dimers (**12a**−**f**, **13**−**19**). R and R′ groups are defined in Table 1. Synthesis of **19** is described in the text and Supporting Information. Reagents and conditions for the reactions are as follows: (a) Cs_2CO_3, alkyl or acyl halide, anh DMF; (b) TBDMSCl, imidazole, DMF; (c) NBS, CCl_4; (d) Cs_2CO_3, **2**, DMF; (e) KF, CH_3COOH, DMF; (f) Et_3N/SO_3, CH_3CN/DMF (4:1), microwave; (g) Me_3Al, R-H, toluene; (h) Cs_2CO_3, **1a**, DMF; (i) LAH, anh THF; (j) Cs_2CO_3, morpholine, DMF; (k) Cs_2CO_3, **4a**, DMF; (l) Cs_2CO_3, DMF, desilylated **8a**; (m) alc LiOH. See text for details.

desilylation and sulfation gave **17**, which is also a disulfated dimer but with a structure completely different from **16**. Likewise, another variant of disulfated dimer, i.e., **18**, was synthesized by coupling **1a** and **2a** in five steps (Figure 2). In combination, dimers **15**−**18** display anionic groups around three key positions (3, 5, and 6) of the benzofuran scaffold. These contain either two or three negative charges, which approximate the number of charges typically found on a heparin disaccharide.

Thrombin Inhibition Potential of Designed Sulfated Benzofuran Monomers and Dimers. Inhibition of thrombin by the designed benzofurans was measured through Spectrozyme TH hydrolysis assay, as described earlier.[18,19] This assay relies on the decrease in the initial rate of substrate hydrolysis in the presence of the sulfated benzofuran derivative as a quantitative measure of the inhibition. The fractional decrease in initial rate of hydrolysis typically shows a sigmoidal profile on a semilog plot, which is

dx.doi.org/10.1021/jm2005767 |J. Med. Chem. 2011, 54, 5522–5531

fitted by dose−response eq 1 to derive IC_{50}, HS, Y_0, and Y_M parameters for each potential inhibitor.

Figure 3 shows the semilog inhibition curves observed for selected benzofuran monomers and dimers. Of the 28 potential inhibitors studied in this work, only 11 molecules exhibited reasonable inhibition of human α-thrombin at pH 7.4 and 25 °C. These included sulfated monomer **5i** and dimers **12a**−**f**, **13**, and **17**−**19** (Tables 1 and 2). Within this group, inhibitors **12b**, **12c**, and **12f** were the only molecules exhibiting IC_{50} less than 50 μM. The *tert*-butyl derivative **12c** was found to be the most potent thrombin inhibitor with an IC_{50} of 7.3 μM under physiologically relevant conditions.

The range of inhibition efficacy was found to vary considerably with the structure of the inhibitor. For example, sulfated dimer **12e** displayed essentially complete inhibition of thrombin (95%, Table 2) while dimer **15** with two carboxylic acid groups inhibited to the extent of only 14% (Table 2). Nearly 85% of the inhibitors studied inhibited thrombin to more than 60%, suggesting good overall efficacy in this series of sulfated benzofurans.

Comparison of the two series of benzofuran molecules shows that dimers tend to inhibit thrombin several-fold better than monomers. Of the 15 sulfated monomers studied in this work and 17 sulfated and unsulfated monomers studied earlier,[23] only **5i** inhibited thrombin with measurable potency (~500 μM, Table 1). By contrast, most sulfated dimers displayed thrombin inhibition (Table 2). This suggested that an oligomeric scaffold may exhibit higher potency and rationalizes the nanomolar potency observed for sulfated LMWL inhibition of thrombin.[18]

The distinct groups at the 2, 3, 5, and 6 positions on the benzofuran ring result in interesting structure−activity relationships. The sulfate group at the 5 position was found to be the key basis for thrombin inhibition, since all unsulfated precursors studied in this work, monomers as well as dimers, did not inhibit thrombin. Such high level of dependence on one sulfate group is striking. It also appears to be unusual because thrombin is known to be considerably forgiving in recognizing ligands. For example, ligands as different as heparin and RNA are known to bind in

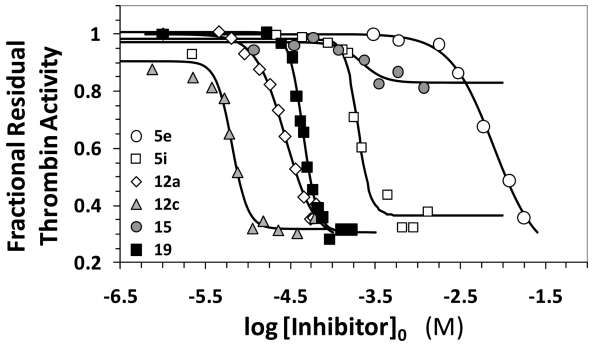

Figure 3. Direct inhibition of thrombin by designed sulfated benzofuran monomers and dimers. The inhibition of human thrombin was determined spectrophotometrically through a Spectrozyme TH hydrolysis assay at pH 7.4 and 25 °C. Solid lines represent sigmoidal fits to the data to obtain IC_{50}, Y_M, and Y_0 (eq 1), as described in the Experimental Procedures. See text for details.

Table 2. Inhibition of Human α-Thrombin by Sulfated Benzofuran Dimers[a]

	R	R′	log IC_{50} (M)	IC_{50} (μM)	ΔY
12a	$-OCH_2CH_3$	$-CH_3$	-4.22 ± 0.16[b]	60 ± 22	0.75
12b	$-OCH_3$	$-CH_3$	-4.43 ± 0.12	37 ± 11	0.68
12c	$-OC(CH_3)_3$	$-CH_3$	-5.14 ± 0.18	7.3 ± 3.1	0.84
12d	$-OCH_2CH_2OCH_3$	$-CH_3$	-3.42 ± 0.13	375 ± 109	0.80
12e	$-OCH_2CH_3$	$-CH_2CH_3$	-3.92 ± 0.05	121 ± 14	0.95
12f	$-OCH_2CH_3$	$-CH(CH_3)_2$	-4.52 ± 0.19	30 ± 13	0.72
13	na[c]	na[c]	-3.89 ± 0.20	129 ± 60	0.62
14	*N*-morpholino	$-CH_3$	incomplete[d]	>7100	na[c]
15	−OH	$-CH_3$	-3.43 ± 0.37	~374[e]	0.14
17	na[c]	na[c]	-3.12 ± 0.35	~764[e]	0.95
18	na[c]	na[c]	-3.44 ± 0.06	365 ± 57	0.79
19	na[c]	na[c]	-4.05 ± 0.26	89 ± 54	0.70

[a] Thrombin inhibition was measured in spectrophotometric assay through initial rate of Spectrozyme TH hydrolysis as described in Experimental Procedures. [b] Standard error shown is ±1 SE. [c] Not applicable. See complete structures of **13**, **14**, **15**, **17**, **18**, and **19** in Figure 2. [d] Full inhibition profile was not measured. [e] The error in IC_{50} could not be accurately defined because of insufficient number of data points.

Table 1. Inhibition of Human α-Thrombin by Sulfated Benzofuran Monomers[a]

compd	R	R′	log IC_{50} (M)	IC_{50} (μM)	ΔY
5a	$-OCH_2CH_3$	$-CH_3$	nd[b]	>2500[c]	
5b	$-OCH_3$	$-CH_3$	nd[b]	>3000[c]	
5c	$-OC(CH_3)_3$	$-CH_3$	nd[b]	>3000[c]	
5d	$-OCH_2CH_2OCH_3$	$-CH_3$	nd[b]	>2000[c]	
5e	$-OCH_2CH_3$	$-CH_2CH_3$	-1.7 ± 0.2[d]	20560 ± 8500	0.60
5f	$-OCH_2CH_3$	$-CH(CH_3)_2$	-1.9 ± 0.3	13650 ± 10400	0.75
5g	$-OCH_2CH_3$	$-CH_2OCH_3$	nd[b]	>16000[c]	
5h	$-OCH_2CH_3$	morpholine-4-carbonyl	nd[b]	>25000[c]	
5i	$-OCH_2CH_3$	benzoyl-*p*-methoxy	-3.3 ± 0.2	520 ± 280	0.54
5j	$-OCH_2CH{=}CH_2$	$-CH_3$	nd[b]	>3000	
9a	*N*-morpholino	$-CH_3$	nd[b]	>2000[c]	
9b	*N*-piperidino	$-CH_3$	nd[b]	>2000[c]	
10[e]	$-CH_2CH_3$	$-CH_3$	nd[b]	>7000[c]	

[a] Thrombin inhibition was measured in spectrophotometric assay through initial rate of Spectrozyme TH hydrolysis as described in Experimental Procedures. [b] Not determined because of incomplete and/or poor inhibition. [c] Estimates on the basis of the highest concentration used in experiment. [d] Standard error shown is ±1 SE. [e] **10** contains a morpholine group at the allylic position (instead of a $-CH_3$ group). See Figure 2 for the full structure.

dx.doi.org/10.1021/jm2005767 |*J. Med. Chem.* 2011, 54, 5522–5531

exosite II.[31,32] Similarly, hirudin, which contains a sulfated tyrosine, and desulfated hirudin, i.e., desirudin, bind in exosite I with excellent affinities.[2,10,13,33]

The stringent requirement for 5-sulfate led to the expectation that multiple sulfate groups on the benzofuran scaffold may induce higher potency. Yet dimers **17** and **18**, which bear two sulfate groups (5 and 5′, and 5 and 6 positions, respectively) inhibited thrombin approximately 6- to 17-fold weaker (Table 2). Furthermore, the IC_{50} of **15**, which contains the 5-sulfate as well as a carboxylate at each of the 3-positions of the benzofuran rings, also decreases 6.2-fold from its parent **12a**. This implies that any additional anionic group on the benzofuran scaffold is counterproductive, which is contrary to what one would predict on the basis of the thrombin−heparin system.[17,31,32]

Comparison of IC_{50} of **12a**, **12b**, and **12c** shows that as lipophilicity of the 3-ester increases, the inhibition potency improves 8.2-fold (Table 2). Likewise, change in substitution from ethyl to isopropyl at the 6-position, as in **12e** and **12f**, also increases the potency nearly 4-fold. This implies that hydrophobicity of the scaffold plays an important role in thrombin recognition. In support of this, increase in hydrophilicity of groups markedly decreases potency. For example, the 3-methoxyethyl ester containing **12d** is a 6.2-fold weaker inhibitor of thrombin than 3-ethyl containing **12a** (Table 2). More importantly, introduction of an *N*-morpholinyl ring (dimer **14**) increased IC_{50} to >2000 μM, which represents a more than 270-fold loss of affinity from a comparable *tert*-butyl ester containing dimer **2c**.

While the above discussion suggests fairly stringent structural requirements on the benzofuran scaffold, two interesting results highlight the possible variances. Dimer **13** containing a morpholine ring at the 2-allylic position displays IC_{50} of 129 μM, which is only 2.2-fold higher than that of **12a**. This suggests that introduction of a hydrophilic and sterically bulkier group at the terminus opposite the 5-sulfate is not detrimental. Likewise, dimer **19** displays no change in IC_{50} from its comparable parent **12a** (Table 2). Dimer **19** contains a 2-CH_2O-6 intermonomeric linkage compared to a 2-CH_2O-5 linkage present in dimer **12a**. An essentially identical inhibition potency of **19** compared to **12a** indicates that a change as drastic as a ring flip, or regioisomerism, is well tolerated.

Mechanism of Thrombin Inhibition by Sulfated Benzofuran Dimer 12a. To elucidate the nature of thrombin inhibition by the designed sulfated benzofurans, the kinetics of Spectrozyme TH hydrolysis by thrombin at pH 7.4 in the presence and absence of **12a** was studied. Spectrozyme TH has been routinely used as a chromogenic substrate of thrombin.[18] The initial rate of amidolysis as a function of the substrate concentration displayed a hyperbolic profile, as expected (Figure 4), from which the Michaelis constant (K_M) and maximal velocity of the reaction (V_{MAX}) were derived. The K_M and V_{MAX} for Spectrozyme TH in the absence of **12a** was found to be 18.9 μM and 100 mAU min^{-1} μM^{-1}, respectively. In the presence of 1.5, 3.0, 10.5, and 30 μM **12a**, the K_M of substrate was found to be 12.6 ± 4.7, 15.5 ± 5.5, 15.9 ± 7.4, and 15.5 ± 3.7 μM. In contrast, the V_{MAX} was measured to be 97 ± 13, 107 ± 14, 73 ± 13, and 66 ± 6 mAU min^{-1} μM^{-1} in these experiments. This corresponds to ∼34% decrease in maximal velocity of reaction upon approximately 50% saturation of the enzyme. This suggests that the presence of **12a** does not significantly affect the binding of the chromogenic substrate to the active site of the enzyme while significantly reducing its catalytic efficiency.

The above Michaelis−Menten kinetics result indicates a noncompetitive, allosteric mechanism of thrombin inhibition by **12a** and, by analogy, other sulfated benzofuran molecules. The reduction in catalytic efficiency by these novel inhibitors is primarily brought about by the slow conversion of the thrombin−Spectrozyme TH Michaelis complex, which may arise from the intrinsic change in the rate of chemical reaction or by a change in the structure of the catalytic triad induced by the allosteric inhibitors.

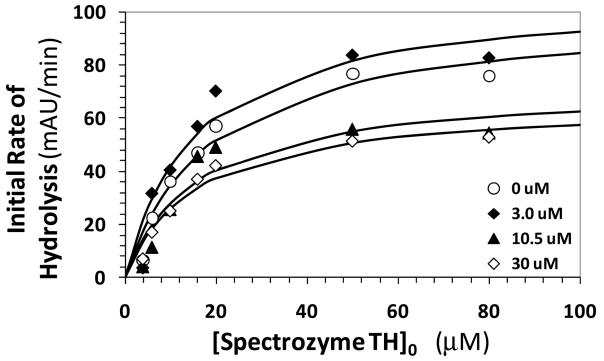

Figure 4. Michaelis−Menten kinetics of Spectrozyme TH hydrolysis by human thrombin in the presence of dimer **12a**. The initial rate of hydrolysis at various substrate concentrations was measured spectrophotometrically in pH 7.4 buffer as described in Experimental Procedures. The concentrations of **12a** chosen for study include 0 (○), 3.0 (◆), 10.5 (▲), and 30 μM (◇). Solid lines represent nonlinear regressional fits to the data by the standard Michaelis−Menten equation to yield K_M and V_{MAX}.

Prolongation of Plasma Clotting Time by Sulfated Benzofurans. Two plasma clotting assays are typically used to assess the anticoagulant potential of new coagulation inhibitors. These are the prothrombin and activated partial thromboplastin time assays (PT and APTT, respectively), which attempt to measure the effect of an inhibitor on the extrinsic and intrinsic flux of coagulation. The concentrations of the inhibitors required to double the PT and APTT were measured, as described earlier for sulfated LMWLs.[20,21] The prolongation of plasma clotting time as a function of the concentration of the sulfated benzofurans followed a pattern typical of other well-studied anticoagulants (Figure 5) except for the range of active concentrations. A 2-fold increase in PT required 850−2100 μM concentration of **5i**, **12a**, or **12b** (Table 3). In a similar manner, the doubling of APTT required 355−1250 μM **5i**, **12a**, **12c**, or **12e** (Table 3). Most other monomers or dimers were found to be not effective. These results suggest that the designed small, sulfated benzofurans are about 100- to 250-fold less potent in human plasma than the oligomeric sulfated LMWLs from which they were designed.[21] This is not too unexpected considering that thrombin inhibition by the smaller synthetic molecules is nearly 400-fold weaker than that of the parent oligomers. Yet interesting similarities and differences are discernible. For example, dimers are better anticoagulants in plasma than monomers. Within the group of dimers, **12a**, **12c**, and **12e**, which inhibit thrombin well, are also the best in terms of prolonging APTT. Interestingly, **12b**, which is comparable to **12a** in thrombin inhibition, does not affect APTT at all (Table 3), and the reason for this behavior is not clear. Overall, the plasma studies suggest the feasibility of designing sulfated benzofurans that will function as anticoagulants in vivo.

■ SIGNIFICANCE

The range of thrombin inhibition potency and efficacy discovered for sulfated benzofurans suggest that the designed sulfated

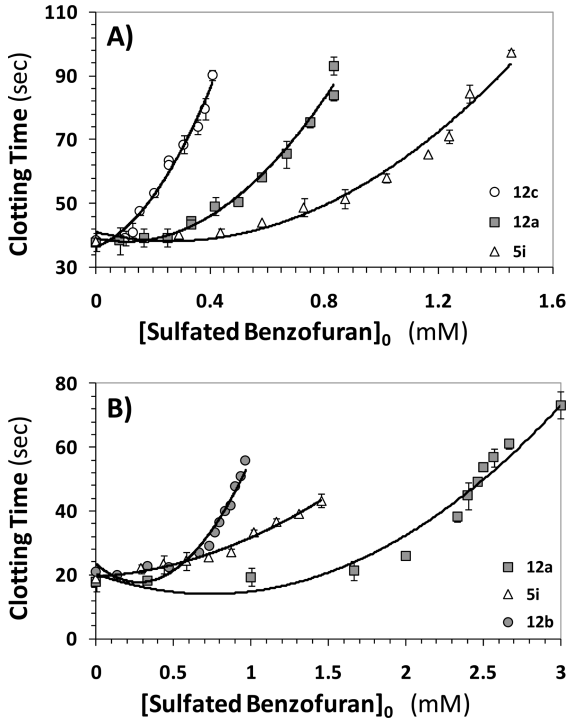

Figure 5. Prolongation of clotting time as a function of concentration of sulfated benzofuran monomers and dimers in either activated partial thromboplastin time assay (A) or prothrombin time assay (B). Solid lines are trend lines and not nonlinear regressional fits. Error bars in the range of symbol size have been omitted. APTT and PT assays were performed as described in the Experimental Procedures.

Table 3. Effect of Designed Sulfated Benzofurans on Human Plasma Clotting Time[a]

compd	APPT (μM)	PT (μM)
5i	1250	1200
5g	>1200	ne[b]
5c	>2000	ne[b]
12a	740	2100
12b	>1000	850
12c	355	ne[b]
12d	>1000	ne[b]
12e	530	ne[b]
14	>1000	nd[c]
15	>1000	ne[b]

[a] PT and APTT values were deduced in in vitro human plasma experiments where the clot initiator is either thromboplastin or ellagic acid, respectively. See Methods section for details. [b] No effect. [c] Not determined.

benzofuran scaffold may be an excellent lead in developing anticoagulants radically different from those studied to date. The $\beta-5$ intermonomer linkage is only one of the many units present in sulfated LMWLs,[18,21] which implies that computational structure-based design may be necessary to identify the most appropriate "small" structure from the large number of potential molecules. One such strategy, e.g., combinatorial virtual library screening, has been put forward for highly sulfated molecules[34] and also been found useful for sulfated lignins binding to antithrombin.[25]

This work presents small, synthetic, sulfated aromatic structures as novel allosteric modulators of thrombin function. Although it is too early to speculate on the site of binding of sulfated benzofurans, the parent oligomeric sulfated LMWLs are known to engage exosite 2 of thrombin.[18] Allosteric, exosite 2-based modulators of thrombin are of special interest because they afford the possibility of controlled inhibition of this key protease that takes part in a number of physiological processes.[13] Excess inhibition could, in principle, be reversed by highly sulfated small molecules, e.g., sucrose octasulfate, that are also expected to bind in this region without inducing significant reduction in thrombin's catalytic activity. Allosteric, exosite 2-mediated inhibitors with nanomolar potency, other than sulfated LMWLs,[18] have not been designed as yet, and thus, sulfated benzofurans represent first molecules in a new class of thrombin modulators.

Although the potency of our first allosteric inhibitors is not high, it is not a major concern because rational design of these molecules from the parent polymers invoked a rather drastic reduction in molecular weight. Whereas sulfated LMWLs are oligomeric chains with an average molecular weight of 5000, sulfated benzofurans range from 500 to 1000.[21] Thus, a relatively easy approach to higher potency would be to prepare appropriate trimers and tetramers of sulfated benzofurans.

Finally, this work also highlights the opportunity of exploring allosteric modulators of other coagulation enzymes, e.g., factors Xa, IXa, and XIa, through sulfated lignin scaffolds. Considering the wealth of structural diversity accessible with the lignin scaffold, it may be possible to design allosteric inhibitors that target these enzymes in a highly specific manner.

■ ASSOCIATED CONTENT

Supporting Information. Synthesis and spectral properties of molecules depicted in Figure 2. This material is available free of charge via the Internet at http://pubs.acs.org.

■ AUTHOR INFORMATION

Corresponding Author

*Address: Department of Medicinal Chemistry, Virginia Commonwealth University, 800 East Leigh Street, Suite 212, P.O. Box 980133, Richmond, VA 23219. Phone: 804-828-7328. Fax: 804-827-3664. E-mail: urdesai@vcu.edu.

■ ACKNOWLEDGMENT

This work was supported by Grants HL099420 and HL090586 from the National Institutes of Health. We thank Dr. H. Tonie Wright for helpful discussions and reading of the manuscript.

■ ABBREVIATIONS USED

APTT, activated partial thromboplastin time; LMWL, low molecular weight lignin; PT, prothrombin time

■ REFERENCES

(1) Bauer, K. A. New anticoagulants. *Hematology (Am. Soc. Hematol., Educ. Program Book)* **2006**, 450–456.

(2) Henry, B. L.; Desai, U. R. Anticoagulants. In *Burger's Medicinal Chemistry, Drug Discovery and Development*, 7th ed.; Abraham, D. J., Rotella, D. P., Eds.; John Wiley: Hoboken, NJ, 2010; pp 365–408.

(3) Straub, A.; Roehrig, S.; Hillisch, A. Oral, direct thrombin and factor Xa inhibitors: the replacement of warfarin, leeches and pig intestines? *Angew. Chem., Int. Ed.* **2011**, *50*, 4574–4590.

(4) Steinmetzer, T; Sturzebecher, J. Progress in the development of synthetic thrombin inhibitors as new orally active anticoagulants. *Curr. Med. Chem.* **2004**, *11*, 2297–2321.

(5) Saiah, E.; Soares, C. Small molecule coagulation cascade inhibitors in the clinic. *Curr. Top. Med. Chem.* **2005**, *5*, 1677–1695.

(6) Smallheer, J. M.; Quan, M. L. Recent advances in coagulation serine protease inhibitors. *Annu. Rep. Med. Chem.* **2009**, *44*, 189–208.

(7) Tucker, T. J.; Brady, S. F.; Lumma, W. C.; Lewis, S. D.; Gardell, S. J.; Naylor-Olsen, A. M.; Yan, Y. W.; Sisko, J. T.; Stauffer, K. J.; Lucas, B. J.; Lynch, J. J.; Cook, J. J.; Stranieri, M. T.; Holahan, M. A.; Lyle, E. A.; Baskin, E. P.; Chen, I. W.; Dancheck, K. B.; Krueger, J. A.; Cooper, C. M.; Vacca, J. P. Design and synthesis of a series of potent and orally bioavailable noncovalent thrombin inhibitors that utilize nonbasic groups in the P1 position. *J. Med. Chem.* **1998**, *41*, 3210–3219.

(8) Burgey, C. S.; Robinson, K. A.; Lyle, T. A.; Nantermet, P. G.; Selnick, H. G.; Isaacs, R. C. A.; Lewis, S. D.; Lucas, B. J.; Krueger, J. A.; Singh, R.; Miller-Stein, C.; White, R. B.; Wong, B.; Lyle, E. A.; Stranieri, M. T.; Cook, J. J.; McMasters, D. R.; Pellicore, J. M.; Pal, S.; Wallace, A. A.; Clayton, F. C.; Bohn, D.; Welsh, D. C.; Lynch, J. J.; Yan, Y. W.; Chen, Z. G.; Kuo, L.; Gardell, S. J.; Shafer, J. A.; Vacca, J. P. Pharmacokinetic optimization of 3-amino-6-chloropyrazinone acetamide thrombin inhibitors. Implementation of P3 pyridine *N*-oxides to deliver an orally bioavailable series containing P1N-benzylamides. *Bioorg. Med. Chem. Lett.* **2003**, *13*, 1353–1357.

(9) Brånalt, J.; Gustafsson, D.; Nilsson, I.; Polla, M. New Heterocyclic Carboxamides for Use as Thrombin Inhibitors. Int. Pat. Appl. WO 2009/157860 A1, 2009; AstraZeneca AB.

(10) Liu, L. W.; Vu, T. K.; Esmon, C. T.; Coughlin, S. R. The region of the thrombin receptor resembling hirudin binds to thrombin and alters enzyme specificity. *J. Biol. Chem.* **1991**, *266*, 16977–16980.

(11) Hortin, G. L.; Trimpe, B. L. Allosteric changes in thrombin's activity produced by peptides corresponding to segments of natural inhibitors and substrates. *J. Biol. Chem.* **1991**, *266*, 6866–6871.

(12) Ye, J.; Liu, L. W.; Esmon, C. T.; Johnson, A. E. The fifth and sixth growth factor-like domains of thrombomodulin bind to the anion-binding exosite of thrombin and alter its specificity. *J. Biol. Chem.* **1992**, *267*, 11023–11028.

(13) Huntington, J. A. Molecular recognition mechanisms of thrombin. *J. Thromb. Haemostasis* **2005**, *3*, 1861–1872.

(14) Monteiro, R. Q.; Rapôso, J. G.; Wisner, A.; Guimarães, J. A.; Bon, C.; Zingali, R. B. Allosteric changes of thrombin catalytic site induced by interaction of bothrojaracin with anion-binding exosites I and II. *Biochem. Biophys. Res. Commun.* **1999**, *262*, 819–822.

(15) Monteiro, R. Q. Targeting exosites on blood coagulation proteases. *An. Acad. Bras. Cienc.* **2005**, *77*, 275–280.

(16) Li, W.; Johnson, D. J.; Adams, T. E.; Pozzi, N.; De Filippis, V.; Huntington, J. A. Thrombin inhibition by serpins disrupts exosite II. *J. Biol. Chem.* **2010**, *285*, 38621–38629.

(17) Olson, S. T.; Halvorson, H. R.; Bjork, I. Quantitative characterization of the thrombin−heparin interaction. Discrimination between specific and nonspecific binding models. *J. Biol. Chem.* **1991**, *266*, 6342–6352.

(18) Henry, B. L.; Monien, B. H.; Bock, P. E.; Desai, U. R. A novel allosteric pathway of thrombin inhibition. Exosite II mediated potent inhibition of thrombin by chemo-enzymatic, sulfated dehydropolymers of 4-hydroxycinnamic acids. *J. Biol. Chem.* **2007**, *282*, 31891–31899.

(19) Henry, B. L.; Abdel Aziz, M.; Zhou, Q.; Desai, U. R. Sulfated, low molecular weight lignins are potent inhibitors of plasmin, in addition to thrombin and factor Xa: novel opportunity for controlling complex pathologies. *Thromb. Haemostasis* **2010**, *103*, 507–515.

(20) Henry, B. L.; Thakkar, J. N.; Martin, E. J.; Brophy, D. F.; Desai, U. R. Characterization of the plasma and blood anticoagulant potential of structurally and mechanistically novel oligomers of 4-hydroxycinnamic acids. *Blood Coagulation Fibrinolysis* **2009**, *20*, 27–34.

(21) Monien, B. H.; Henry, B. L.; Raghuraman, A.; Hindle, M.; Desai, U. R. Novel chemo-enzymatic oligomers of cinnamic acids as direct and indirect inhibitors of coagulation proteinases. *Bioorg. Med. Chem.* **2006**, *14*, 7988–7998.

(22) Raghuraman, A.; Riaz, M.; Hindle, M.; Desai, U. R. Rapid, high-yielding microwave-assisted per-sulfation of organic scaffolds. *Tetrahedron Lett.* **2007**, *48*, 6754–6758.

(23) Verghese, J.; Liang, A.; Sidhu, P. S.; Hindle, M.; Zhou, Q.; Desai, U. R. First steps in the direction of synthetic, allosteric, direct inhibitors of thrombin and factor Xa. *Bioorg. Med. Chem. Lett.* **2009**, *19*, 4126–4129.

(24) Liang, A.; Thakkar, J. N.; Desai, U. R. Study of physico-chemical properties of novel highly sulfated, aromatic, mimetics of heparin and heparan sulfate. *J. Pharm. Sci.* **2010**, *99*, 1207–1216.

(25) Henry, B. L.; Connell, J.; Liang, A.; Krishnasamy, C.; Desai, U. R. Interaction of antithrombin with sulfated, low molecular weight lignins. Opportunities for potent, selective modulation of antithrombin function. *J. Biol. Chem.* **2009**, *284*, 20897–20908.

(26) Pei, L.; Li, Y.; Bu, X.; Gu, L.; Chan, A. S. C. One-pot synthesis of 5,6-dihydroxylated benzo[*b*]furan derivatives. *Tetrahedron Lett.* **2006**, *47*, 2615–2618.

(27) Al-Horani, R. A.; Desai, U. R. Chemical sulfation of small molecules—advances and challenges. *Tetrahedron* **2010**, *66*, 2907–2918.

(28) Basha, A.; Lipton, M.; Weinreb, S. A mild, general method for conversion of esters to amides. *Tetrahedron Lett.* **1977**, *48*, 4171–4174.

(29) Flessner, T.; Doye, S. Cesium carbonates: a powerful inorganic base in organic synthesis. *J. Prakt. Chem.* **1999**, *341*, 186–190.

(30) Dayal, B.; Salen, G.; Toome, B.; Tint, G. S.; Shefer, S.; Padia, J. Lithium hydroxide/aq. methanol: a mild reagent for hydrolysis of bile acids methyl esters. *Steriods* **1990**, *55*, 233–237.

(31) Carter, W. J.; Cama, E.; Huntington, J. A. Crystal structure of thrombin bound to heparin. *J. Biol. Chem.* **2005**, *280*, 2745–2749.

(32) Jeter, M. L.; Ly, L. V.; Fortenberry, Y. M.; Whinna, H. C.; White, R. R.; Rusconi, C. P.; Sullenger, B. A.; Church, F. C. RNA aptamer to thrombin binds anion-binding exosite-2 and alters protease inhibition by heparin-binding serpins. *FEBS Lett.* **2004**, *568*, 10–14.

(33) Liu, C. C.; Brustad, E.; Liu, W.; Schultz, P. G. Crystal structure of a biosynthetic sulfo-hirudin complexed to thrombin. *J. Am. Chem. Soc.* **2007**, *129*, 10648–10649.

(34) Raghuraman, A.; Mosier, P. D.; Desai, U. R. Finding needle in a haystack. Development of a combinatorial virtual screening approach for identifying high specificity heparin/heparan sulfate sequence(s). *J. Med. Chem.* **2006**, *49*, 3553–3562.